Using Elemental Se and Ag to Grow Pure Ag$_2$Se Dendrites/Dendritic-Films of Highly Oriented (001) Nanocrystals

Dapeng Li,[†] **Zhi Zheng,**[*,†,‡] **Zhengyang Shui,**[†] **Mingqiang Long,**[†] **Jie Yu,**[‡] **Ka Wai Wong,**[†,‡] **Lin Yang,**[§] **Lizhi Zhang,**[*,∥] **and Woon Ming Lau**[‡,⊥]

Institute of Surface Micro and Nano Materials, Xuchang University, Xuchang, Henan Province 461000, PR China, Department of Physics, The Chinese University of Hong Kong, Shatin, N. T., PR China, College of Chemistry and Environmental Science, Henan Normal University, Xinxiang 453007, PR China, Key Laboratory of Pesticide & Chemical Biology of Ministry of Education, College of Chemistry, Central China Normal University, Wuhan 430079, PR China, and Surface Science Western, The University of Western Ontario, London, Ontario, Canada

A clean, facile route of using only common bulk selenium (Se) powder and silver (Ag) foil in a simple solvothermal process is developed to synthesize a film of silver selenide (Ag$_2$Se) dendrites of highly oriented (001) nanocrystals. The simple process takes ~10 h at 160 °C in a common alcohol such as methanol or ethanol in an autoclave, and the reaction time is shorter than in many prevalent methods. The adoption of elemental Se and Ag (foil) in the synthesis eases the control of the purity of the product, simplifies the reaction steps, and reduces the costs, as the synthesis does not require Se and Ag compounds, and also requires no chemical additives other than an alcohol as solvent. The results support a mechanism of dissolution of the bulk-like Se powder in the solvothermal process, transport of solvated Se to react with Ag, nucleation of Ag$_2$Se nanocrystals, surface-mediated, solvation-assisted surface diffusion of Ag$_2$Se nanocrystals, and diffusion-limited aggregation of the Ag$_2$Se nanocrystals through oriented attachment for the growth of dendrites having highly oriented (001) nanocrystals. The clean, relative facile route is practical for the fabrication of Ag$_2$Se crystals/films with hierarchically ordered nanostructures for future applications in solar cell devices. More importantly, the same concept can be adopted for the synthesis of other nanomaterials with bulk elemental reactants with no reliance on chemical compounds or additives.

Introduction

The current rapid development of nanoscience and nanotechnology for producing nanosized semiconductor materials demands further development of novel nanomaterials with well-defined morphologies and improved properties.[1–7] To transfer the science and technology to practical production, the development of simple synthesis methods to reduce the number of reaction steps and the reliance on chemical additives is required for yield and cost control. In this context, a variety of synthesis methods have been developed to prepare nanocrystalline silver selenide (Ag$_2$Se) because this promising A$^I_2$B^{VI} semiconductor can be used to make solar cells,[8] magnetic field sensors,[9] solid-state electrochemical sensors,[10] and optical filters.[11] Prevalent synthesis methods include the use of microwave radiation,[12] sonochemical force,[13] microemulsion mixing,[14] and electrochemical potential[15] to drive the decomposition of selenium and/or silver compounds to form Ag$_2$Se. To promote the growth of specific, desirable nanocrystalline morphology, various molecular precursors, additives, and surfactants are introduced.[16–18] Recent attractive examples of new developments in the synthesis of nanocrystals of Ag$_2$Se include reports by Qian and co-workers

in which Ag$_2$Se tubular crystals[19] and chainlike Ag$_2$Se nanorods inside carbonaceous nanotubes were prepared by a hydrothermal method by using N$_2$H$_4$·H$_2$O as the reaction medium.[20] Several groups have demonstrated the synthesis of Ag$_2$Se nanowires by templating against nanowires of trigonal Se in an aqueous colloidal system with AgNO$_3$ as the silver source.[21–24] In addition, Ng et al. prepared Ag$_2$Se nanowires by using ultraviolet light to decompose CSe$_2$ as the Se source and Ag nanowires as the template.[25] At least two research groups[26,27] have also shown the formation of Ag$_2$Se nanocrystals by fluxing selenium and sodium sulfite to form selenosulfate, which is then mixed with AgNO$_3$ in concentrated aqueous ammonium. Although all of these approaches have been demonstrated to yield Ag$_2$Se with interesting nanocrystalline morphology, the demands of process simplification continue to push for novel technology development. In current nanomaterials studies, researchers have recognized that crystalline semiconductors with different morphologies may exhibit different physical and chemical properties even if their chemical compositions are the same.[28,29] For example, in applications of nanoscale semiconductors as solar cell devices, 2D or 3D nanostructures or nanowebs are more attractive than 1D nanorods or nanowires because they can transport holes or electrons more effectively via the interconnected networks in the 2D and 3D scaffolds.[30] The formation of dendritic 2D and 3D scaffolds is particularly attractive because the 3D dendritic morphology provides both the electrical links and a high surface/volume ratio.[30] Generally, templates or shape-directing surfactants play important roles in construct-

* Address correspondence to these authors. (Z.Z.) E-mail: zhengzhi9999@yahoo.com.cn. (L.Z.) E-mail: zhanglz@mail.ccnu.edu.cn.
† Xuchang University.
‡ The Chinese University of Hong Kong.
§ Henan Normal University.
∥ Central China Normal University.
⊥ The University of Western Ontario.

Figure 1. Representative TEM images of (a) an individual dendrite of Ag$_2$Se and (b) the corresponding SAED pattern recorded from a branch tip.

Figure 2. XRD pattern of the Ag$_2$Se film prepared in the Se/alcohol system at 160 °C for 12 h with an Se concentration of 6.67 × 10^{-4} g/mL.

Figure 3. EDX spectrum recorded from a nanorod (branch of a dendrite) grown on the surface of a stem at 160 °C for 12 h with an Se concentration of 6.67 × 10^{-4} g/mL.

products, and raises production costs. All of these considerations make the development of novel, practical synthesis approaches for fabricating hierarchically ordered 2D or 3D dendritic nanostructures of Ag$_2$Se challenging.

In this article, we present a very simple reaction strategy for the in-situ fabrication of crystalline Ag$_2$Se dendrites of highly oriented (001) nanocrystals. The reaction design adopts the recent confirmation by Xie et al.[33] that although the solubility of elemental Se in ordinary conditions is known to be extremely low, Se can dissolve in a simple solvothermal process at 160 °C in a variety of common organic solvents. The design further adopts the recently known results of Ag$_2$Se formation when elemental Se and Ag are in contact,[34] particularly the recent report on Ag$_2$Se dendrite formation on Ag nanowires by UV decomposition of CSe$_2$ to supply Se.[25] The combination of these two design concepts leads to our new method of using a simple solvothermal process to dissolve elemental Se powder in alcohol and transport the solvated Se to an Ag foil for the formation of nanocrystalline Ag$_2$Se dendrites. In preparing Ag$_2$Se crystals of high purity and without further posttreatment, metal salts and other templates or shape-directing surfactants are eliminated in our reaction design.[35] This design strategy is expected to yield the simplest chemical synthesis of hierarchically ordered nanocrystalline Ag$_2$Se. This article reports on the realization of such an experimental design, the characterization of the nanocrystalline Ag$_2$Se dendrites thus formed, and the possible reaction mechanisms.

Experimental Section

Synthesis. All reagents were of analytical grade. In a typical procedure, a piece of silver foil (Sinopharm Chemical Reagent Co., Ltd, purity >99.9%, thickness 0.1 mm, 3 cm × 0.5 cm), 0.01 g of selenium powder (Aldrich), and 15 mL of ethanol (or methanol or dodecanol) were placed in a 20 mL Teflon-lined autoclave. The autoclave was maintained at 160 °C for 12 h and cooled in air to room temperature. The silver foil was taken out of the solution and washed with ethanol several times and then air dried for characterization. For further investigation of the crystal-formation process, some experiments were performed with different reaction times and cooling processes.

Characterization. X-ray diffraction (XRD) patterns were recorded using a Philips MPD 18801 diffractometer using Cu Kα radiation. Scanning electron microscopy (SEM) measurements were performed using a JSM-5600 SEM with an energy-dispersive X-ray fluorescence analyzer. The nanostructures and selected-area electron diffraction (SAED) patterns

ing 2D and 3D nanostructures.[18,31,32] For example, work by Ng et al., which has been cited in the preceding paragraph, shows the growth of Ag$_2$Se dendrites from Ag nanowires as a growth template, with the decomposition of CSe$_2$ used to feed the growth. However, as discussed earlier, the introduction of surfactants, templates, or catalysts complicates the synthesis process, increases the risk of leaving impurities in the final
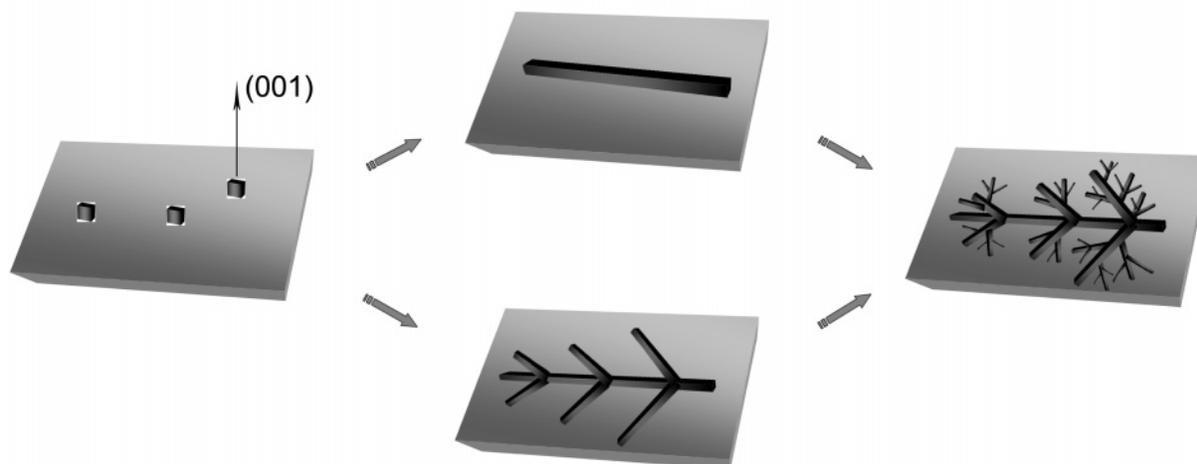
Figure 4. Schematic diagrams of the Ag$_2$Se dendrite growth mechanisms. (Scheme A) Growth from an Ag nanowire with no surface-mediated support. (Scheme B) Growth from an Ag foil surface with surface-mediated nucleation and diffusion to enable (001)-oriented dendrite growth.

of the resulting Ag$_2$Se dendrite were recorded by transmission electronmicroscopy (TEM, Philips CM120).

Results and Discussion

Evidence of the Formation of Dendrites of Ag$_2$Se Nanocrystals. When the synthesis is conducted with either methanol or ethanol as the solvent and the amount of Se load is kept at a low level of ~7 × 10^{-4} g/mL (0.01 g/15 mL), dendrites of Ag$_2$Se nanocrystals are formed, with each dendritic branch often in single-crystal form and nearly all branches having their (001) crystal directions pointing along the surface normal of the Ag foil substrate. A representative TEM image of an individual dendrite obtained from the Se/methanol system is shown in Figure 1a. In this image, the diameter of the dendritic branches is roughly ~50 nm. The selected-area electron diffraction (SAED) pattern shown in Figure 1b represents the crystallinity of one dendritic branch and confirms the nature of a single crystal. The pattern can be indexed to the diffraction spots of orthorhombic β-Ag$_2$Se, which is indeed the most common crystal phase of Ag$_2$Se at room temperature. In this work, we have not observed any other crystal phases with TEM or XRD, phases including the cubic α-Ag$_2$Se phase that should be the stable phase at $T > 133$ °C and has been recently observed as a metastable phase at room temperature.

The above dendrites are present in the form of a thin film on the Ag foil substrate. Figure 2 shows the representative XRD pattern of a typical Ag$_2$Se film prepared with the Se/alcohol system at 160 °C for 12 h with an Se concentration of 6.67 × 10^{-4} g/mL. The appearance of (111) and (200) reflections originating from the silver substrate (JCPDS card, no. 87-720)

indicates that the resulting Ag$_2$Se film is thin. All of the other peaks can be indexed to the (002), (112), (121), (013), and (004) planes of the orthorhombic β-Ag$_2$Se (JCPDS card, no. 24-1041, space group P212121), except some weak reflections that come from a trace amount of condensed and unreacted elemental Se. It is expected that the presence of this residual elemental Se can be eliminated by either decreasing the original load of Se powder or prolonging the reaction time. On the whole, the XRD results indicate that the resulting Ag$_2$Se dendrites/film are dominated by β-Ag$_2$Se crystals with their (001) directions preferentially aligned with the normal direction of the Ag foil substrate. As such, the β-Ag$_2$Se crystals are highly ordered with such a preferred orientation. The composition of the dendritic film is shown to have the stoichiometry of Ag$_2$Se by energy-dispersive X-ray spectroscopy (EDX) microanalysis. No other undesirable components can be found. The results taken from a dendrite branch are shown in Figure 3.

Possible Mechanisms for the Growth of Dendrites of Highly Oriented β-Ag$_2$Se (001) Nanocrystals. The observed formation of β-Ag$_2$Se on Ag foil is no doubt the result of the dissolution of the Se powder, the transportation of the solvated Se to the Ag foil, and the production of Ag$_2$Se via the Se−Ag reaction. The dissolution process of Se has already been confirmed and discussed elsewhere.[33] The production of β-Ag$_2$-Se by mixing elemental Se and Ag is also known, for example, Ag$_2$Se can be formed by the sequential deposition of Se and Ag ultrathin layers[36] or the deposition of Se on the Ag film.[34] Hence, the clarification of the mechanisms for the observed β-Ag$_2$Se growth should focus on the driving forces for the
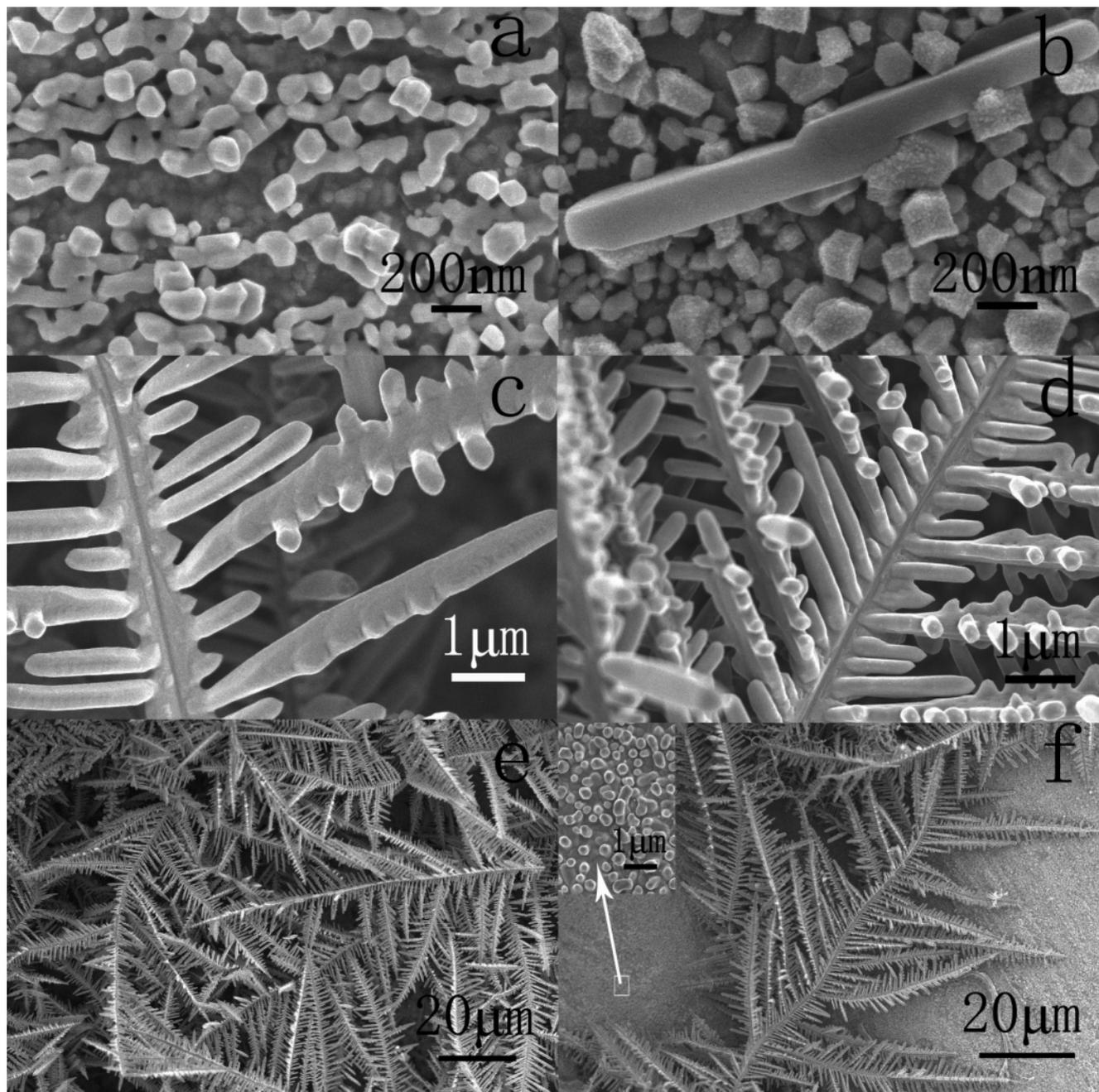
Figure 5. SEM morphologies: (a) nanocrystals of (001)-oriented Ag$_2$Se (orientation confirmed by XRD) after 1 h of solvothermal growth with methanol as the solvent; (b) oriented attachment toward the formation of the trunk of a dendrite after 3 h of solvothermal growth with methanol as the solvent; (c) closeup of a full dendrite formed after 12 h of solvothermal growth with methanol as the solvent; (d) closeup of a full dendrite formed after 12 h of solvothermal growth with dodecanol as the solvent; (e) large-field view of dendrites formed under the conditions of part c for the case of a relatively high nucleation density; and (f) large-field view of dendrites formed under the condition of part d for the case of a relatively low nucleation density.

formation of dendrites of highly oriented β-Ag$_2$Se (001) nanocrystals.

The formation of dendrites of β-Ag$_2$Se nanocrystals was recently reported by Ng et al., who grew the dendrites by decomposing CSe$_2$ with UV irradiation in the presence of Ag nanowires. According to their proposed mechanism of dendrite formation, the arrival of Se at an Ag nanowire leads to the formation of Ag$_2$Se. In the aging duration of 14 days at room temperature, the Ag$_2$Se reaction product aggregates first into nanoparticles that are possibly solvated. The diffusion and diffusion-limited aggregation of these nanoparticles give rise to the formation of dendrites from an Ag nanowire, which is graphically depicted in Figure 4a.

In the context of dendrite formation through the well-known diffusion-limited aggregation process,[37,38] one member of our research group has also explained the formation of highly oriented (001) graphite dendrites on Cu (111).[39] In this case, which can be used as a growth model to explain the dendrites of highly oriented β-Ag$_2$Se (001) nanocrystals that are present, carbon atoms are implanted into a Cu (111) crystal and are then driven out back to the surface via thermal annealing. Because carbon does not react chemically with copper, carbon atoms arriving on the Cu(111) surface form graphite clusters with their basal planes oriented parallel to the Cu(111) surface because of surface-energy minimization. These highly oriented (001) graphite clusters then diffuse on the surface, which can be

Films of Highly Oriented Nanocrystals

J. Phys. Chem. C, Vol. 112, No. 8, 2008 **2849**

described as surface-mediated diffusion. The diffusion-limited aggregation of the graphic clusters produces dendrites of highly oriented (001) graphite clusters. This prior knowledge combined with the known results of dendrite formation of β-Ag$_2$Se (001) nanocrystals on an Ag nanowire (Figure 4a) leads to the following proposed mechanism of our observation of a film of dendrites of highly oriented β-Ag$_2$Se (001) nanocrystals on a silver foil (Figure 4b).

Similar to the case of dendrite formation of β-Ag$_2$Se nanocrystals on a silver nanowire, the formation of β-Ag$_2$Se nanocrystals on a silver foil also follows the mechanism comprising the arrival of Se on the silver surface, the formation of Ag$_2$Se, and the nucleation of β-Ag$_2$Se nanocrystals.

Different from the formation of β-Ag$_2$Se nanocrystals on a silver nanowire, the formation of β-Ag$_2$Se nanocrystals on a silver foil is supported by surface-energy minimization toward the formation of β-Ag$_2$Se nanocrystals with their (001) crystal orientation preferentially aligned with the normal direction of the flat surface. Furthermore, the diffusion of the β-Ag$_2$Se nanocrystals is also mediated by the flat surface, which leads to the tendency of forming 2-D dendrites parallel to the flat surface initially. During this growth, the known oriented attachment (OA) mode[40] for the growth of a single-crystal microstructure by the condensation of nanocrystals drives the formation of the observed single-crystal nature of the β-Ag$_2$Se dendrite branches (Figure 1). The diffusion of β-Ag$_2$Se nanocrystals on top of this first layer of 2-D dendrites leads to the growth of the dendritic film in a 3-D island growth mode. The growth morphology is thus fundamentally different from that for dendrite formation of β-Ag$_2$Se nanocrystals on a silver nanowire (Figure 4a vs b).

Direct evidence of the proposed 3-D island growth mechanism of the observed dendrite formation of highly oriented (001) β-Ag$_2$Se nanocrystals (Figure 1) is shown in Figure 5 which gives the evolution of the dendrites of highly oriented (001) β-Ag$_2$Se nanocrystals as a function of the solvothermal reaction time. Briefly, when the solvothermal reaction is aborted after 1 h, the formation of separated (001) β-Ag$_2$Se nanocrystals on the silver foil is the domain feature of the growth process (Figure 5a). After the solvothermal reaction for 3 h, single crystal "trunks" such as that at the center of Figure 5b are formed via surface-mediated diffusion and the oriented attachment of (001) β-Ag$_2$Se nanocrystals. Finally, after the solvothermal reaction for 12 h, various dendrite forms are formed (Figure 5c,d and Supporting Information). Impressively, all of them exhibited well-defined, hierarchically ordered dendritic structures that consist of a long central trunk (several tens of micrometers in length) with highly ordered secondary and tertiary branches (nanorods). It is important to note that such dendrite-like hierarchical nanostructures can always be obtained in high yield within a large reaction area (3 cm × 0.5 cm, shown in Figure 5e,f), with side branches emerging at about 60 angles with respect to the central trunk. Interestingly, when dodecanol was selected, the resulting Ag$_2$Se product exhibited a large, perfect dendrite with hierarchically ordered secondary and tertiary nanostructures (Figure 5f), and the length of the main stem of the dendrite can reach a very high value of 100 μm. The inset of Figure 5f shows the magnified image of an area free of dendritic structures, which mainly shows the Ag$_2$Se nanoparticles (about 100$-$200 nm in diameter). The results indicate that the nucleation and growth with dodecanol as a solvent are much slower than those of more polar solvents such as methanol and ethanol. This is likely related to the differences in solvation of Se and Ag$_2$Se by different solvents.

In this work, dendrites of β-Ag$_2$Se nanocrystals with different morphologies have been fabricated by fine tuning the growth conditions. The influential attributes include the Se concentration (adjusted by the Se powder load), the solvent, the temperature and the duration of the solvothermal process. In general, increasing the Se concentration accelerates the growth but promotes secondary nucleation during the initial formation of the β-Ag$_2$Se seed nanocrystals and dendrite formation. Hence, although a film comprising dendrites of β-Ag$_2$Se nanocrystals can be formed in less than 10 h, the growth of highly oriented (001) β-Ag$_2$Se nanocrystals in the dendrites cannot be maintained. Instead, the resultant dendrites have random grain orientations. In addition, the solvent selection also affects the dendrite morphology as illustrated by the differences between the morphology associated with dodecanol and those associated with methanol and ethanol. Furthermore, although both alcohols and benzene are known to support the dissolution of Se powder in a solvothermal process[33] and have indeed been used successfully in this work for the growth of β-Ag$_2$Se on a silver foil, only alcohols, not benzene, can be used successfully to form dendritic structures of highly oriented (001) β-Ag$_2$Se nanocrystals (Supporting Information). Apparently, the proper solvation of the β-Ag$_2$Se nanocrystals and the substrate surface during dendrite formation are also critical.

Conclusions

The film formation through the 3D island growth of dendrites of highly oriented (001) β-Ag$_2$Se nanocrystals has been demonstrated. The growth reaction merely requires the load of bulk elemental Se powder and silver in the form of a foil or a film on any substrate carrier, in a simple solvothermal process with a common alcohol as the solvent. The growth is facile, with film formation occurring in ~10 h. No other compounds or chemical additives are required. We advocate it as a practical method for the development of novel nanostructures of Ag$_2$Se and other related selenide materials. In addition, we have also completed the feasibility test of using this method for generating nanodendritic Ag$_2$Se as a substrate for matrix-assisted laser-induced ionization mass spectrometry of organic and biochemical molecules. Preliminary results showed that with the use of our nanodendritic Ag$_2$Se layers, biological macromolecules (e.g., cholesterol, which is difficult to analyze by traditional MALDI-MS) can be successfully ionized, desorbed, and detected with relative ease without the need for organic matrices commonly employed in MALDI-MS.

Supporting Information Available: SEM morphologies of Ag$_2$Se dendrites generated from different solvents. This material is available free of charge via the Internet at http://pubs.acs.org.

References and Notes

(1) Cozzoli, P. D.; Comparelli, R.; Fanizza, E.; Curri, M. L.; Agostiano, A.; Laub, D. *J. Am. Chem. Soc.* **2004**, *126*, 3868.

2850 *J. Phys. Chem. C, Vol. 112, No. 8, 2008*

Li et al.

(2) Pagba, C.; Zordan, G.; Galoppini, E.; Piatnitski, E. L.; Hore, S.; Deshayes, K.; Piotrowiak, P. *J. Am. Chem. Soc.* **2004**, *126*, 9888.

(3) Hinds, S.; Taft, B. J.; Levina, L.; Sukhovatkin, V.; Dooley, C. J.; Roy, M. D.; MacNeil, D. D.; Sargent, E. H.; Kelley, S. O. *J. Am. Chem. Soc.* **2006**, *128*, 64.

(4) Zhan, J. H.; Bando, Y.; Hu, J. Q.; Liu, Z. W.; Yin, L. W.; Golberg, D. *Angew. Chem., Int. Ed.* **2005**, *44*, 2140.

(5) Selvan, S. T.; Patra, P. K.; Ang, C. Y.; Ying, J. Y. *Angew. Chem., Int. Ed.* **2007**, *46*, 2448.

(6) Shen, G. Z.; Bando, Y.; Ye, C. H.; Yuan, X. L.; Sekiguchi, T.; Golberg, D. *Angew. Chem., Int. Ed.* **2006**, *45*, 7568.

(7) Dong, L. Q.; Hollis, T.; Connolly, B. A.; Wright, N. G.; Horrocks, B. R.; Houlton, A. *Adv. Mater.* **2007**, *19*, 1748.

(8) Lakshmikumar, S. T.; Rastogi, A. C. *Sol. Energy Mater. Sol. Cells* **1994**, *32*, 7.

(9) Mogwitz, B.; Gruhl, F.; Kreutzbruck, M. V.; Korte, C.; Janek, J. *Z. Anorg. Allg. Chem.* **2004**, *630*, 1744.

(10) Schown, D. T.; Xie, C.; Cui, Y. *J. Am. Chem. Soc.* **2007**, *129*, 4116.

(11) Liang, Y. C.; Tada, K. *J. Appl. Phys.* **1988**, *64*, 4494.

(12) Manoharan, S. S.; Prasanna, S. J.; Kiwitz, D. E.; Schneider, C. M. *Phys. Rev. B* **2001**, *63*, 212405.

(13) Zhan, J. H.; Yang, X. G.; Li, S. D.; Wang, D. W.; Xie, Y.; Qian, Y. T. *Int. J. Inorg. Mater.* **2001**, *3*, 47.

(14) Buschmann, V.; Tendeloo, G. V.; Monnoyer, P.; Nagy, J. B. *Langmuir* **1998**, *14*, 1528.

(15) Becdelie, A. M.; Amosse, J.; Barbier, M. J. *Mater. Res. Bull.* **1970**, *5*, 367.

(16) Stuczynski, S. M.; Brennan, J. G.; Steigerwald, M. L. *Inorg. Chem.* **1989**, *28*, 4431.

(17) Cheon, J.; Zink, J. I. *J. Am. Chem. Soc.* **1997**, *119*, 3838.

(18) Zhang, L. Z.; Yu, J. C.; Mo, M. S.; Wu, L.; Li, Q.; Kwong, K. W. *J. Am. Chem. Soc.* **2004**, *126*, 8116.

(19) Hu, J. Q.; Deng, B.; Lu, Q. Y.; Tang, K. B.; Jiang, R. R.; Qian, Y. T.; Zhou, G. E.; Cheng, H. *Chem. Commun.* **2000**, *715*.

(20) Ma, D. K.; Zhang, M.; Xi, G. C.; Zhang, J. H.; Qian, Y. T. *Inorg. Chem.* **2006**, *45*, 4845.

(21) Gates, B.; Wu, Y. Y.; Yin, Y. D.; Yang, P. D.; Xia, Y. N. *J. Am. Chem. Soc.* **2001**, *123*, 11500.

(22) Zhang, S. Y.; Fang, C. X.; Wei, W.; Jin, B. K.; Tian, Y. P.; Shen, Y. H.; Yang, J. X.; Gao, H. W. *J. Phys. Chem. C* **2007**, *111*, 4168.

(23) Jiang, Z. Y.; Xie, Z. X.; Zhang, X. H.; Huang, R. B.; Zheng, L. S. *Chem. Phys. Lett.* **2003**, *378*, 313.

(24) Gates, B.; Mayers, B.; Wu, Y. Y.; Sun, Y. G.; Cattle, B.; Yang, P. D.; Xia, Y. N. *Adv. Funct. Mater.* **2002**, *12*, 679.

(25) Ng, C. H. B.; Tan, H.; Fan, W. Y. *Langmuir* **2006**, *22*, 9712.

(26) Pejova, B.; Najdoski, M.; Grozdanov, I.; Dey, S. K. *Mater. Lett.* **2000**, *43*, 269.

(27) Batabyal, S. K.; Basu, C.; Das, A. R.; Sanyal, G. S.; Banerjee, D.; Bandyopadhyay, N. R. *Mater. Manufact. Proc.* **2006**, *21*, 694.

(28) Kelly, N. E.; Lee, S. O.; Harris, K. D. M. *J. Am. Chem. Soc.* **2001**, *123*, 12682.

(29) Hulliger, J. *Angew. Chem., Int. Ed. Engl.* **1994**, *33*, 143.

(30) Gur, I.; Fromer, N. A.; Chen, C. P.; Kanaras, A. G.; Alivisatos, A. P. *Nano Lett.* **2007**, *7*, 409.

(31) Zhang, L. Z.; Ai, Z. H.; Jia, F. L.; Liu, L.; Hu, X. L.; Yu, J. C. *Chem.—Eur. J.* **2006**, *12*, 4185.

(32) Xiao, J. P.; Xie, Y.; Tang, R.; Luo, W. *J. Mater. Chem.* **2002**, *12*, 1148.

(33) Lu, J.; Xie, Y.; Xu, F.; Zhu, L. Y. *J. Mater. Chem.* **2002**, *12*, 2755.

(34) Safran, G.; Geszti, O.; Radnoczi, G.; Barna, P. B. *Thin Solid Films* **1998**, *317*, 72.

(35) Zheng, Z.; Liu, A. R.; Wang, S. M.; Wang, Y.; Li, Z. S.; Lau, W. M.; Zhang, L. Z. *J. Mater. Chem.* **2005**, *15*, 4555.

(36) Ohtani, T.; Maruyama, K.; Ohshima, K. *Mater. Res. Bull.* **1997**, *32*, 343.

(37) Witten, T. A.; Sander, L. M. *Phys. Rev. Lett.* **1981**, *47*, 1400.

(38) Daccord, G.; Nittmann, J.; Stanley, H. E. *Phys. Rev. Lett.* **1986**, *56*, 336.

(39) Huang, L. J.; Lau, W. M. *J. Phys.: Condens. Matter* **1993**, *5*, 7087.

(40) Cheng, Y.; Wang, Y. S.; Chen, D. Q.; Bao, F. *J. Phys. Chem. B* **2005**, *109*, 794.